# Reverse Remodeling of Tricuspid Valve Morphology and Function in Chronic Thromboembolic Pulmonary Hypertension Patients Following Pulmonary Thromboendarterectomy – A Cardiac Magnetic Resonance Imaging and Invasive Hemodynamic Study

**Christian Alcaraz Frederiksen** ( caf@clin.au.dk )
Aarhus University Hospital Department of Cardiology: Arhus Universitetshospital Hjertesygdomme
https://orcid.org/0000-0001-6583-2885
**Farhad Waziri**
Aarhus University Hospital
**Steffen Ringgaard**
Aarhus University Hospital
**Søren Mellemkjær**
Aarhus University Hospital
**Tor Skibsted Clemmensen**
Aarhus University Hospital
**Vibeke Elisabeth Hjortdal**
Rigshospitalet
**Sten Lyager Nielsen**
Aarhus University
**Steen Hvitfeldt Poulsen**
Aarhus University Hospital

**Research article**

**Keywords:** Cardiac magnetic resonance imaging, Tricuspid valve, Chronic thromboembolic pulmonary hypertension

**Posted Date:** August 4th, 2021

**DOI:** https://doi.org/10.21203/rs.3.rs-331545/v2

# Abstract

*Background*

To investigate changes in tricuspid annulus (TA) and tricuspid valve (TV) morphology among chronic thromboembolic pulmonary hypertension (CTEPH) patients before and 12 months after pulmonary thromboendarterectomy (PEA) and compare these findings to normal control subjects.

*Methods*

20 CTEPH patients and 20 controls were enrolled in the study. The patients were examined with echocardiography, right heart catherization and cardiac magnetic resonance imaging prior to PEA and 12 months after.

*Results*

Right atrium (RA) volume was significantly reduced from baseline to 12 months after PEA (30 ±9 versus 23 ±5ml/$m^2$, p<0.005). TA base area in systole remained unchanged (p=0.11) and was comparable to controls. The leaflet area, tenting volume and tenting height in systole were significantly increased at baseline but decreased significantly with comparable values to controls after 12 months (p<0.005). There was correlation between the changes of right ventricular-pulmonary artery coupling and changes of TV tenting height (r = -0.54, p=0.02), TV tenting volume (r = -0.73, p<0.001) and TV leaflet area (-0.57, p = 0.01) from baseline to 12 months after PEA.

Tricuspid regurgitation jet area/RA area was significantly (p<0.01) reduced from baseline (30 ±13%) to 12 months after PEA (9 ±10%).

*Conclusions*

In CTEPH patients selected for PEA, TV tenting height, volume and valve area are significantly increased whereas annulus size and shape are less affected. The alterations in TV morphology are fully reversed after PEA and correlates to improvements of right ventricular-pulmonary arterial coupling.


# Background

Functional tricuspid regurgitation (TR) is one of the most frequent manifestations of heart valve disease. It develops as a consequence of geometrical distortion in the anatomical structures situated in relation to the tricuspid valve (TV) causing leaflet tethering and tricuspid annular (TA) dilatation [1]. Functional TR is often secondary to left sided valve disease or chronic atrial fibrillation [2, 3]. Pulmonal arterial hypertension (PH) is another important cause of functional TR that might lead to excessive right ventricle (RV) remodeling and dysfunction. The subsequent annular and atrial dilatation with development of right sided heart failure carries a poor prognosis [4, 5]. Reduction of PH is associated with TR severity regression in contrast to progression of PH that is associated with an increase of TR severity which is

associated with poor survival [6]. In patients with worsening PH progressive TR development is shown to relate to RV enlargement and increased RV sphericity leading to TA dilatation and increased TV tethering [6]. Patients with chronic thromboembolic pulmonary hypertension (CTEPH) suffer from varying degrees of functional TR in combination with right sided heart failure. Following successful pulmonary thromboendarterectomy (PEA) an immediate dramatic reduction in pulmonary artery (PA) pressures is often seen [7, 8]. Early post-operative examination by two-dimensional (2D) echocardiography and right heart catherization have demonstrated that reduction in PA systolic pressures after PEA is associated with a significant 70% reduction in the number of patients with severe TR. This reduction occurs despite of persistent tricuspid annular dilation [8]. However, the long-term effects on TR severity and detailed changes in TV morphology in relation to changes of pulmonary pressures, RV-PA coupling, and RV/TA remodeling have not been studied in detail. The assessment of RV and TV function including evaluation of TR severity is routinely performed by 2D echocardiographic examination which has some limitations due to the inherent geometrical anatomic characteristics of the right side of the heart [9]. Transthoracic three-dimensional (3D) echocardiography offers accurate data on RV volumes, function and valve morphology. However, precise 3D echocardiographic imaging of the TV can be technically challenging and is difficult to obtain in all patients. Cardiac Magnetic Resonance Imaging (CMR) is considered as the gold standard for accurate assessment of RV and RA dimension, volumes and function. In addition, the analysis of TV morphology and function by assessment of leaflet tethering, coaptation and TA area or circumference can be obtained by CMR.

In the present study, we aimed to investigate the changes of TA and TV morphology assessed by CMR with relation to changes in pulmonary arterial pressures by right heart catherization (RHC) in CTEPH patients before and 12 months after PEA and compare these findings to normal control subjects.

## Methods

# Patients

Between December 2014 and January 2017, we enrolled 20 CTEPH patients and 20 controls in the study at Aarhus University Hospital, Denmark. In total, 47 consecutive patients were evaluated for CTEPH during the study period. After clinical and diagnostic evaluation 20 patients were identified to fulfill the criteria for participation in in the study [10, 11]. The reasons for exclusion were as follows: five patients declined to participate, five patients did not meet the diagnostic criteria of CTEPH (three idiopathic pulmonary arterial hypertension, one idiopathic pulmonary fibrosis and one with constrictive pericarditis); five patients had only borderline PH and received medical treatment, four patients were deemed inoperable or excluded due to co-existing comorbidities and eight were excluded for various other reasons.

The CTEPH diagnosis was defined in accordance with the World Health Organization classification as PH with a mean PA pressure (mPAP) $\geq$ 25 mmHg, a pulmonary capillary wedge pressure $\leq$ 15 mmHg, and specific angiographic signs at least 3 months after effective anticoagulation [12]. The CTEPH patients

were examined with RHC, transthoracic echocardiography (TTE) and CMR on the same day, prior to PEA and 12 months after PEA. The controls were enrolled from all parts of Denmark through an online recruitment website (forsoegsperson.dk), to ensure that the controls represented the general population. The control group participated on a volunteer basis and prior to inclusion they underwent screening to exclude cardiovascular disease with medical history, ECG, TTE and blood pressure measurement. They were required to be asymptomatic and received no medication. All examinations including CMR was performed on the same day.

The PEA procedure was performed on cardiopulmonary bypass in deep hypothermia and periods of circulatory arrest. None of the patients underwent concomitant coronary artery bypass grafting or valve interventions.

# Cardiac magnetic resonance

CMR was performed using a Philips Achieva dStream 1.5 T whole body MR scanner (Philips Medical Systems, Best, Netherlands). Cine scanning (time-resolved imaging) was used to assess right atrium (RA) and ventricle and left atrium and ventricle volumes and geometry. An integrated 4-electrode electrocardiogram (ECG) was used to synchronize data acquisition. A survey scan was followed by an ECG-triggered temporally resolved cine scan using a balanced steady-state free precession sequence during breath-hold. The following imaging parameters were used: repetition time 2.9ms, echo time 1.46ms, flip angle 90°, 160×136 acquisition matrix, 30 phases within one cardiac cycle, slice thickness 8mm and field of view 319 × 319 mm.

A stack of 3 long-axis slices was acquired for 4-chamber view, and for short-axis view 10–12 slices were acquired covering the entire right and left ventricle. For tricuspid valve analysis a special focused stack specifically designed for this study consisting of 6–8 long-axis slices and 10–12 slices in short-axis were acquired covering the entire tricuspid valve and right ventricle. Pulmonary flow measurements were obtained using a free-breathing, ECG-triggered phase contrast sequence. The image parameters for the phase contrast sequence were: slice thickness 7mm, 301×301mm field of view, 128×96 acquisition matrix, 35 cardiac frames, velocity encoding 150cm/s and scan duration 1:43min. Image analysis of the heart chambers and pulmonary flow were performed using Segment v.2.2 R6274 (Medviso AB, Lund, Sweden). Tricuspid valve analyses were performed in an inhouse software originally developed for detailed mitral valve analyses as described previously [13] (Siswin, Aarhus, Denmark).

Anatomical details of the TV and TA were measured by manually tracing multiple slices through the stack. This allowed for the construction of a 3-dimensional model of the valve and the annulus. The base area was defined by projecting annular points to the same fitted plane. Annular height was defined as the maximal distance away from this plane between annular points. A schematic overview of the measured parameters is illustrated in Fig. 1.

RA area and volume were assessed from 4-chamber view by manual detection of endocardial border. RA length and width were assessed from 4-chamber view by measuring the inner atrial border distance in

longitudinal and transverse direction, respectively. The sphericity index of the RV is estimated in the 4-chamber view as the ratio of the short diameter (RVDd1) and RV length in end-diastole. LV volumes were calculated from the short-axis cine images. From the stack of parallel short-axis images, end-diastolic volume (EDV), end-systolic volume (ESV), and masses were assessed (LV masses in end-diastole and RV masses in end-systole), and stroke volume (SV) and ejection fraction were calculated. RV and LV myocardial masses were assessed from the stack of parallel short-axis images by manual detection of endocardial and epicardial borders on each slice. Cardiac output (CO) was measured as pulmonary flow. CO was indexed to body surface area as cardiac index (CI).

# Transthoracic echocardiography

Transthoracic echocardiography was performed using a Vivid E95 ultrasound system (GE Healthcare, Horten, Norway) equipped with an M5S transducer.

Color Doppler imaging was used to assess severity of the TR, and the transvalvular gradient was measured using continuous-wave Doppler. Quantification of TR severity was done in accordance with guidelines using the proximal isovelocity surface area method and estimation of TR jet area/RA area [9].

The echocardiographic data were blinded to invasive measurements and clinical status and examined by a single investigator. Data were analyzed offline using dedicated software (EchoPAC version 213, GE Healthcare, Horten, Norway).

# Right heart catheterization

Standard RHC was performed using a standard 7.5F triple-lumen Swan-Ganz catheter (Edwards Lifesciences, Irvine, CA, USA). The following parameters were measured: mean RA pressure (mRAP), systolic, diastolic and mPAP, mean pulmonary capillary wedge pressure (PCWP), CO, CI and systemic blood pressure. PCWP was measured at end expiration. CO was measured according to the Fick principle. RV contractility was also quantified by maximum/end-systolic elastance (Ees) and RV afterload with arterial elastance (Ea). Ees was calculated as (RV maximum pressure − mPAP) divided by SV [14, 15]. Ea was estimated by the ratio of mPAP to SV [15]. Since healthy controls were not examined with RHC, RV-pulmonary arterial (PA) coupling was assessed using only the volume method (Ees/Ea = RV-SV/RV-end systolic volume) [15, 16]. For comparison between the CTEPH patient group and healthy control group we used the RV volume method.

# Statistical analysis

Data are presented as mean ± standard deviation, unless otherwise specified. Histograms and Q-Q-plots were used to check for normality. Between-group differences were assessed by t-test for normally distributed data and Mann–Whitney U-test for non-normally distributed data. Baseline versus 12 months differences were assessed by the paired sample t-test and Wilcoxon signed-rank test for non-normally distributed data. Pearson's correlation coefficient was calculated for normally distributed data and Spearman correlation coefficient for non-normally distributed data. Categorical variables were compared using the chi-square test. To test for inter-observer and intra-observer variability, Bland-Altman plots and

interclass correlation coefficient were used. Analyses were performed using Stata (STATA/IC 14.2, StataCorp LP, College Station, TX, USA).

# Results

Baseline characteristics of 20 CTEPH patients and 20 control subjects are shown in Table 1. No patients had ischemic heart disease, one patient had diabetes mellitus, one patient suffered from essential thrombocytosis and one had a Leiden mutation.

Table 1
Patient characteristics

| | Baseline (n = 20) | Controls (n = 20) | P-value |
|---|---|---|---|
| Age (years) | 61 ± 14 | 54 ± 9 | 0.07 |
| Female, n (%) | 13 (65) | 10 (50) | 0.34 |
| BMI (kg/m$^2$) | 28 ± 6 | 24 ± 4 | < 0.05 |
| NYHA I/II/III/IV, n (%) 0/3/16/1(0/15/80/5) | | | |
| Arterial hypertension, n (%) | 9 (45) | | |
| Atrial fibrillation, n (%) | 3 (15) | | |
| COPD, n (%) | 7 (35) | | |
| Diabetes mellitus, n (%) | 1 (5) | | |
| Ischemic heart disease, n (%) | 0 | | |
| Stroke, n (%) | 1 (5) | | |
| Biochemistry<br>NT-ProBNP (ng/l) | 890 [430; 2692] | | |
| Hemoglobin (mmol/l) | 8.9 ± 1.4 | | |
| Creatinine (µmol/l) | 85 ± 19 | | |
| eGFR (ml/min) | 68 ± 14 | | |
| Medicine | | | |
| Warfarin, n (%) | 20 (100) | | |
| Aspirin, n (%) | 2 (10) | | |
| ACE/ATII inhibitor, n (%) | 9 (45) | | |
| Loop-diuretic, n (%) | 5 (25) | | |
| Thiazide, n (%) | 4 (20) | | |
| Spironolactone, n (%) | 2 (10) | | |
| Sildenafil, n (%) | 1 (5) | | |
| Riociguat, n (%) | 1 (5) | | |

Data are presented as an absolute number and (percent) or mean ± standard deviation or median and [interquartile range]. BMI: Body Mass Index, COPD: Chronic obstructive pulmonary disease, NYHA: New York Heart Association

At baseline, CTEPH patients were highly symptomatic with the majority in New York Heart Association (NYHA) class III, Nt-pro-BNP was mildly elevated and renal function preserved. NYHA class improved from 2.9 ± 0.4 to 1.3 ± 0.6 at 12 months after PEA ($p < 0.0001$). A significant reduction in Nt-ProBNP was also observed: preoperatively 890 [430; 2692] ng/l to 239 [141; 375] ng/l at 12 months ($p < 0.005$). Mild TR was noted in 60 % and moderate-severe TR was noted in 40 % of the patients at baseline with an average effective regurgitant orifice (ERO) of 0.30 ±0.30 $cm^2$ and a TR jet area/RA area of 30 ±13 % for all patients. After 12 months only two patients had moderate-severe TR with an ERO of 0.38 $cm^2$ and 0.47 $cm^2$ whereas 18 patients only had trace or mild TR. The TR jet area/RA area was reduced to 9 ±10%, (vs baseline $p < 0.01$) whereas the ERO, due to very mild regurgitation, was not satisfactory obtainable in 15 patients.

# Reverse remodeling of right atrium, ventricle and tricuspid valve during follow-up by CMR

Table 2 demonstrates the variables of RA, RV and TV at baseline, at 12 months after PEA and in 20 control subjects. At baseline, RA volume was significantly increased but normalized after 12 months as compared to controls. Considerable RV remodeling was demonstrated as RV mass index, RV volumes, dimensions and sphericity index decreased significantly and was comparable with control subjects after 12 months. RV ejection fraction was impaired significantly at baseline but despite improvement remained mildly depressed as compared to controls. Cardiac output and index by CMR also improved significantly being comparable to controls 12 months after PEA. The RV-PA coupling also improved significantly but remained impaired as compared to controls.

Table 2
Cardiac magnetic resonance imaging

| | Baseline (n = 19) | 12 months (n = 19) | P-value | Controls (n = 20) |
|---|---|---|---|---|
| **Right atrium** | | | | |
| Volume (mL/$m^2$) | 30 ± 9* | 23 ± 5 | < 0.005 | 23 ± 6 |
| Length (mm) | 57 ± 8 | 56 ± 10 | 0.54 | 53 ± 7 |
| Width (mm) | 57 ± 12* | 46 ± 8 | < 0.005 | 48 ± 9 |
| **Right ventricle** | | | | |
| RVMi (g/$m^2$) | 22 ± 7* | 13 ± 7 | < 0.0001 | 12 ± 3 |
| End-diastolic volume (mL) | 233 ± 74* | 164 ± 50 | < 0.0001 | 172 ± 41 |
| End-systolic volume (mL) | 168 ± 75* | 94 ± 40 | < 0.0005 | 80 ± 23 |
| RVDd1 (mm) | 54 ± 8* | 42 ± 8 | < 0.0001 | 43 ± 5 |
| RVDd2 (mm) | 48 ± 8* | 38 ± 6 | < 0.0001 | 37 ± 4 |
| RV length (mm) | 86 ± 10 | 78 ± 10 | < 0.0001 | 82 ± 8 |
| RV sphericity index | 2.5 ± 0.2* | 2.8 ± 0.5 | < 0.01 | 2.8 ± 0.4 |
| Stroke volume (mL) | 65 ± 22* | 71 ± 21* | 0.15 | 92 ± 19 |
| TV regurgitant volume (mL) | 11 ± 17 | 4 ± 8 | 0.20 | 4 ± 7 |
| Ejection fraction (%) | 30 ± 13* | 44 ± 10* | < 0.001 | 54 ± 20 |
| **Tricuspid valve** | | | | |
| Base area sys ($cm^2$) | 12.6 ± 3.5 | 11.0 ± 3.2 | 0.11 | 12.4 ± 2.6 |
| Base area dia ($cm^2$) | 14.5 ± 4.2 | 11.7 ± 3.9* | 0.06 | 13.5 ± 2.8 |
| Circumference sys (cm) | 15.0 ± 2.6 | 13.9 ±2.8 | 0.18 | 15.0 ± 2.1 |
| Circumference dia (cm) | 16.7 ± 1.9 | 15.9 ± 3.0 | 0.47 | 16.7 ± 1.9 |

Data are presented as mean ± standard deviation.

AP: anterior-posterior, dia: diastolic SL: septal-lateral, sys: systolic Ea: Arterial elastance, Ees: End-systolic elastance,, RV: Right ventricular, PA: Pulmonary artery, RVD1: Basal RV linear dimension at end-diastole, RVD2: Mid-cavity RV linear dimension at end-diastole, RVMi: Right ventricular mass index, SV: Stroke volume, ESV: End-systolic volume.

*p < 0.05 vs. controls

| | Baseline (n = 19) | 12 months (n = 19) | P-value | Controls (n = 20) |
|---|---|---|---|---|
| Annular height sys (cm) | 1.3 ± 0.5* | 1.1 ± 0.3 | < 0.01 | 1.0 ± 0.3 |
| Annular height dia (cm) | 1.3 ± 0.4 | 1.7 ± 0.7 | 0.16 | 1.5 ± 0.4 |
| SL distance sys (cm) | 4.0 ± 0.6 | 3.8 ± 0.6 | 0.08 | 3.7 ± 0.5 |
| SL distance dia (cm) | 4.4 ± 0.6 | 4.2 ± 0.7 | 0.24 | 4.1 ± 0.5 |
| AP distance sys (cm) | 3.9 ± 0.5 | 3.8 ± 0.7 | 0.42 | 4.1 ± 0.5 |
| AP distance dia (cm) | 4.1 ± 0.6 | 3.7 ± 0.8* | 0.08 | 4.2 ± 0.6 |
| Leaflet area sys ($cm^2$) | 20.1 ± 5.8 | 16.2 ± 6.4 | < 0.005 | 16.9 ± 3.7 |
| Tenting volume sys ($cm^3$) | 4.4 ± 2.6* | 1.6 ± 0.9 | < 0.005 | 1.5 ± 0.8 |
| Tenting height sys ($mm^3$) | 11.4 ± 3.9* | 7.0 ± 2.2 | < 0.0005 | 7.0 ± 1.9 |
| Coaptation height (mm) | 4.9 ± 1.1* | 5.8 ± 1.7* | 0.17 | 7.2 ± 1.5 |
| **Pulmonary artery** | | | | |
| Cardiac output (L/min) | 3.9 ± 0.9* | 5.1 ± 1.4 | < 0.005 | 4.9 ± 0.7 |
| Cardiac index (L/min/$m^2$) | 2.3 ± 0.4* | 2.8 ± 0.6 | < 0.005 | 2.6 ± 0.4 |
| **Non-invasive derived RV-PA coupling** | | | | |
| SV (mL) / ESV (mL) | 0.49 ± 0.30* | 0.84 ± 0.31* | p < 0.0001 | 1.19 ± 0.20 |
| Data are presented as mean ± standard deviation. | | | | |
| AP: anterior-posterior, dia: diastolic SL: septal-lateral, sys: systolic Ea: Arterial elastance, Ees: End-systolic elastance,, RV: Right ventricular, PA: Pulmonary artery, RVD1: Basal RV linear dimension at end-diastole, RVD2: Mid-cavity RV linear dimension at end-diastole, RVMi: Right ventricular mass index, SV: Stroke volume, ESV: End-systolic volume. | | | | |
| *p < 0.05 vs. controls | | | | |

The TV size by base area and circumference did not change significantly even though a tendency towards lower base area was noted. The form of the TA expressed by the annulus septal-lateral (SL) and anterior-posterior (AP) dimensions in systole and diastole did not change significantly during follow-up. However, the AP distance in diastole decreased to a lower distance as compared to controls after 12 months. The SL/AP ratio in systole and diastole remained unchanged during follow-up (baseline vs 12 months: diastole: 1.07 ±0.09 vs 1.20 ±0.36, p = 0.26 and systole: 1.06 ±0.19 vs 0.96 ±0.15, p = 0.094). TA height in systole was increased at baseline but decreased significantly during follow-up and was comparable to controls. The difference between height of TA in systole and diastole changed

significantly. At baseline the difference was 0.2 ±5.1 mm compared to -5.8 ±7.0 mm at 12 months, p = 0.028. The systole-diastole difference was comparable to controls (-4.3 ±3.8 mm) at 12 months.

The leaflet area, volume and tenting height in systole were significantly increased at baseline but decreased significantly with comparable values to controls after 12 months (Fig. 2). Coaptation height increased insignificantly and remained lower than controls at 12 months (Fig. 2).

# Right heart catherization hemodynamic parameters at baseline and 12 months post-operatively

Table 3 demonstrates the hemodynamic data at baseline and after 12 months. As expected pulmonary pressures, pulmonary vascular resistance, pulmonary end-systolic elastance, and pulmonary elastance decreased during follow-up. RA mean pressure decreased significantly with borderline elevated pressure after 12 months while PCWP remained unchanged and within normal range.

Table 3
Invasive hemodynamic parameters

| | **Baseline (n = 19)** | **12 months (n = 19)** | **P-value** |
|---|---|---|---|
| **Hemodynamic characteristics** | | | |
| Heart rate (beats/min) | 73 ± 14 | 76 ± 10 | 0.23 |
| Systolic blood pressure (mmHg) | 135 ± 18 | 139 ± 19 | 0.59 |
| Diastolic blood pressure (mmHg) | 92 ± 13 | 87 ± 12 | 0.14 |
| mRAP (mmHg) | 10.5 ± 5.1 | 4.3 ± 4.2 | < 0.05 |
| sPAP (mmHg) | 81 ± 20 | 43 ± 16 | < 0.0005 |
| dPAP (mmHg) | 33 ± 9 | 17 ± 7 | < 0.0001 |
| mPAP (mmHg) | 51 ± 12 | 27 ± 10 | < 0.0005 |
| PCWP mean (mmHg) | 11 ± 3 | 9 ± 4 | 0.21 |
| PVR (Wood Units) | 10.0 ± 4.5 | 3.9 ± 2.5 | < 0.0005 |
| Ees (mmHg/mL) | 0.52 ± 0.29 | 0.23 ± 0.14 | p < 0.0001 |
| Ea (mmHg/mL) | 0.91 ± 0.45 | 0.43 ± 0.25 | p < 0.0005 |
| Cardiac output (L/min) (Fick) | 5.0 ± 2.5 | 5.1 ± 1.5 | 0.91 |
| Data are presented as mean ± standard deviation. | | | |
| dPAP: Diastolic pulmonary arterial pressure, Ea: Arterial elastance, Ees: End-systolic elastance, mPAP: Mean pulmonary arterial pressure, mRAP: Mean right atrial pressure, PCWP: Pulmonary capillary wedge pressure, PVR: pulmonary vascular resistance, sPAP: Systolic pulmonary arterial pressure. | | | |

# Correlations between changes of hemodynamic parameters and tricuspid valve morphology parameters

The changes of selected hemodynamic parameters and changes to TV parameters from baseline to 12 months after PEA are demonstrated in Table 4. The changes of TA expressed by base area in systole and SL correlated moderately but significantly to changes in systolic PAP and pulmonary end systolic elastance. The alterations of RV-PA coupling correlated also significantly to changes of base area in systole and SL. The changes of mean RA pressure correlated significantly to changes in TA circumference. A stronger significant correlation was noted between changes in RV end systolic volume and RA volume on one side and base area in systole on the other.

Table 4
Correlation analyzes

| Hemodynamics | CMR-TV | r | P-value |
|---|---|---|---|
| Δ SPAP | Δ Base Area Systole | -0.53 | < 0.04 |
| Δ SPAP | Δ SL distance | 0.55 | < 0.03 |
| Δ SPAP | Δ Tenting height | 0.10 | 0.70 |
| Δ SPAP | Δ Coaptation height | -0.04 | 0.88 |
| Δ RA | Δ Base area systole | -0.60 | < 0.02 |
| Δ RA | Δ Circumference | -0.60 | < 0.02 |
| Δ RA | Δ Tenting height | -0.10 | 0.70 |
| Δ RA | Δ Coaptation height | -0.04 | 0.88 |
| Δ CO | Δ Coaptation height | -0.58 | < 0.02 |
| Δ Ees | Δ Base area systole | -0.72 | < 0.003 |
| Δ Ees | Δ SL distance | -0.55 | < 0.03 |
| Δ Ees | Δ Base area systole | 0.26 | 0.29 |
| Δ Ees | ΔSL distance | 0.24 | 0.33 |
| ΔRV-PA coupling | Δ Base area systole | -0.50 | 0.04 |
| ΔRV-PA coupling | Δ SL distance | -0.53 | 0.02 |
| ΔRV-PA coupling | Δ Leaflet area systole | -0.57 | 0.01 |
| ΔRV-PA coupling | Δ Tenting volume systole | -0.73 | < 0.001 |
| ΔRV-PA coupling | Δ Tenting height systole | -0.54 | 0.02 |
| ΔRV-PA coupling | Δ Coaptation height | -0.45 | 0.07 |
| ΔRV-ESV | Base area systole | 0.67 | 0.002 |
| ΔRA-Vol | Base area systole | 0.77 | < 0.001 |

CMR-TV are delta values from morphological changes to the TV between baseline and 12 months post-operatively. r is the correlation coefficient. SPAP: Systolic pulmonary arterial pressure, CO: Cardiac output, SL: septal-lateral, Ees: End-systolic elastance, RA: Right atrium, RV: Right ventricular, PA: Pulmonary artery, ESV: End-systolic volume.

Changes of TV morphology denoted by tenting volume in systole, tenting height in systole and especially tenting volume in systole correlated significantly to changes of RV-PA coupling.

# Discussion

We present, to our knowledge, the first study of TA and TV morphology assessed by CMR combined with additional invasive hemodynamic assessment in patients with severe PH due to chronic pulmonary thromboembolism during 12 months follow-up after PEA. We also provide CMR data on TA and TV morphology in normal subjects.

The main findings were as follows: Firstly, significant changes of TV morphology, noted as leaflet area, tenting volume and tenting height in systole, were significantly reduced but TV parameters were comparable to control subjects after 12 months following PEA; secondly the TA size by circumference and area were without significant changes and were comparable to control subjects. However, the shape of the TA did change significantly as the annulus circularity index (SL/AP-ratio) decreased; thirdly, the TA height in systole decreased significantly and reached comparable values as compared to control subjects; fourthly, the changes to TV morphology expressed by leaflet area, tenting volume and tenting height in systole was significantly and negatively correlated to the changes in RV-PA coupling; finally, as expected significant RV and RA remodeling and improvement of RV systolic function were noted after PEA but the changes to RV and RA dimensions or volumes did not correlate to the changes of the TV morphology observed.

Preoperatively 40 % of our patients demonstrated a moderate-severe functional TR in accordance with observations in PH in which severe TR varies between 10–30 % of cases [2, 17]. As expected we also noted a significant reduction of moderate-severe TR with the presence of only 10 % after 12 months following PEA in accordance with a previous study [8]. Tenting height is reported to be increased in TR with different etiology of PH as demonstrated by Topilsky et al. who reported a tenting height of 8.0 mm assessed by transthoracic 2D echocardiography [18]. The preoperative tenting height was significantly increased to an average of 11.4 mm by CMR (average normal subjects 7.0 mm) which normalized with a height of 7.0 mm after 12 months following PEA. In the present study, the tenting volume of the TV was increased nearly 3-fold preoperatively compared to controls (1.5 $cm^3$) but normalized at follow-up. Increased tenting volume has been reported in patients with functional TR in two previous 3D echocardiographic studies showing a tenting volume of 4.2 $cm^3$ in 17 chronic PH patients with significant TR and of 3.2 $cm^3$ among 53 patients with severe TR and PH of different etiology, respectively [19, 20]. Despite different imaging techniques the tenting volume seems consistently to increase considerably in PH patients with functional TR independent of etiology. Preoperatively, we noted that the leaflet area was increased in systole to the same extent as demonstrated by Afilalo et al. in a study with patients with severe functional TR and PH. In the present study, the leaflet area was significantly decreased and normalized during follow-up[17]. The coaptation height did increase but insignificantly and remained lower than controls at follow-up. The changes in TV morphological parameters were significantly correlated to the changes of RV-PA coupling but was not directly correlated to changes of the annulus, shape nor RV volume or even the sphericity index. The tricuspid leaflet closure depends mainly on leaflet adaptation, tethering forces and annular morphology. Leaflet adaptation is abnormal before PEA but the adaptation seems to reverse to near normal conditions at follow-up. A dramatic RV remodeling was shown after PEA as RV volume, and the sphericity index normalized during follow-up.

Dilatation and changes of RV geometry are known to affect the position and function of the papillary muscles (PM) resulting in increased tethering of the TV [21]. Distortion of the spatial relationships between the RV, PM and TV is likely to influence the presence of TR and the demonstrated changes of the TV morphology and function. However, the major determinants of TR severity have previously been investigated by 3D echocardiography showing that leaflet area, tenting volume and leaflet closure are independent predictors of TR whereas RV dilatation or echocardiographic Doppler estimated systolic pulmonary artery pressure was not [20]. In accordance with the present findings a previous study has shown that regression of TR in PH patients is associated to the changes of TV tethering with reduction in tenting height and area as the major determinants [6].

Previous two- and three-dimensional echocardiographic studies of functional TR in PH patients have reported various degree of TA dilation depending on the severity of the regurgitation [19–21].

Among the present patients no significant increase in annular area or circumference were noted and the annulus size was comparable to control subjects. One important reason for this finding could be that the TR severity of the present population was preoperatively only moderate and thereby contributing less to RA volume overload with subsequent dilatation of the RA as well as the annulus. The potential pathophysiological mechanism in the present patient population is likely to be initiated by the remodeling of the RV and tethering of the TV as seen in other etiologies of PH [19, 22]. In the PH population with TR the TA is often less dilated as compared to patients with secondary functional TR and chronic atrial fibrillation [23, 24]. Despite that the size of the TA seems to be less affected in the present study. Minor but significant changes were noted regarding the annular shape as annular circularity index was increased preoperatively as compared to controls. The minor changes observed in the TA in terms of base area and septal-lateral dimension were modest but significantly correlated to changes in systolic PAP, RV-PA coupling, RV end systolic volume and RA volume. Based on the present data a conservative approach with respect to tricuspid annuloplasty in CTEPH undergoing PEA even with a significant TR seems to be advisory. In patients undergoing left valve disease surgery - in particular mitral valve repair or replacement – tricuspid annuloplasty is recommended when the TA diameter ≥ 40 mm [25].

Preoperatively, our CMR data demonstrated classic RV remodeling as seen in PH with increased RV mass, severe RV dilatation, increased sphericity and impairment of systolic function in terms of reduced ejection fraction and stroke volume. During follow-up, extensive reverse remodeling was noted as RV mass and size were significantly reduced and normalized. However, the RV systolic function remained mildly impaired as compared to controls.

Beyond reporting serial data on RV volume and systolic function, we were able to measure and characterize the TA and TV morphology in CTEPH patients and normal subjects by CMR. The CMR technique seems promising for TV evaluation. The benefit of CMR in the initial diagnosis of CTEPH is probably limited. However, in terms of RV characterization CMR provides very accurate estimates of RV volumes, RV function and TV regurgitant volumes. In addition, LGE and T1-mapping will probably provide insights on RV damage among CTEPH patients in the near future.

In terms of medical treatment for CTEPH there is no clear support for treatment with specific PH active drugs before PEA. Furthermore, the only approved drug in CTEPH, riociguat, is only registered for use in inoperable cases or in persistent PH after PEA [26].

Some limitations have to be considered in the present study. First of all, the number of patients studied is small but the examinations were performed prospectively and consecutively combining CMR techniques with invasively assessed hemodynamic parameters during a complete one year of follow-up. Despite the small number of patients studied as compared to other observational studies of TR and TV in PH patients, we had the opportunity to study the valve morphology in a situation where the hemodynamic conditions were reversed and thereby being able to study the associations between RV remodeling, hemodynamic and morphological TV changes.

The number of PH patients with severe TR varies considerably in line with the present findings which limits the possibility to study to what extent the observed changes in TA and TV has on the patients with severe TR.

# Conclusion

TV tenting height, volume and valve area are significantly increased whereas annulus size and shape are less effected in CTEPH patients selected for PEA when assessed by CMR. The TV morphology alterations were fully reversed and correlated to the demonstrated improvements of RV-PA coupling after PEA during 12 months of follow-up. The present data calls for further studies to evaluate the surgical strategy in CTEPH patients scheduled for PEA, as it may be possible to refrain from annuloplasty in selected cases.

# Abbreviations

TR
tricuspid regurgitation, TV:tricuspid valve; TA:tricuspid annulus; PH:pulmonal arterial hypertension; RV:right ventricle; CTEPH:chronic thromboembolic pulmonary hypertension; PEA:pulmonary thromboendarterectomy; PA:pulmonary artery; CMR:cardiac magnetic resonance imaging; RHC:right heart catherization; mPAP:mean PA pressure; TTE:transthoracic echocardiography; ECG:electrocardiogram; RA:right atrium; EDV:end-diastolic volume; ESV:end-systolic volume; SV:stroke volume; CO:cardiac output; CI cardiac index; NYHA:New York Heart Association; mRAP:mean RA pressure; PCWP:pulmonary capillary wedge pressure; Ees:end-systolic elastance; Ea:arterial elastance; SL:septal-lateral; AP:anterior-posterior.

# Declarations

*Ethics approval and consent to participate*

Patients and controls were ≥18 years of age and included after having provided written informed consent according to the principles of the Helsinki Declaration. The study was approved by The Central Denmark Region Committees on Health Research Ethics (journal number 1-10-72-240-14).

*Consent for publication*

Not applicable.

*Availability of data and materials*

The imaging protocols as well as the datasets used and/or analysed during the current study are available from the corresponding author on reasonable request.

*Competing interests*

The authors declare that they have no competing interests.

*Funding*

This study was funded by the Danish Heart Foundation, Aarhus University, Arvid Nilssons Fond, Eva & Henry Frænkels Mindefond, and Snedkermester Sophus Jacobsen & Hustru Astrid Jacobsens Fond. The funding bodies had no role in study design, data collection, data analysis, data interpretation, and manuscript writing.

*Authors' contributions*

Study design and concept development (FW, SR, SM, TSC, VEH, SLN, SHP); Data aquisition (FW, SM, TSC, SHP); Image analyses (FW, SR, SHP), Statistical analyses (FW), Manuscript draft (CAF, SHP), Interpretation of images and data (CAF, SHP). Critical review and approval of the final manuscript (CAF, FW, SR, SM, TSC, VEH, SLN, SHP).

*Acknowledgements*

Not applicable.

# References

1. Singh JP, Evans JC, Levy D, Larson MG, Freed LA, Fuller DL, et al. Prevalence and clinical determinants of mitral, tricuspid, and aortic regurgitation (the Framingham Heart Study). Am J Cardiol. 1999;83(6):897–902.
2. Mutlak D, Aronson D, Lessick J, Reisner SA, Dabbah S, Agmon Y. Functional tricuspid regurgitation in patients with pulmonary hypertension: is pulmonary artery pressure the only determinant of regurgitation severity? Chest. 2009;135(1):115–21.
3. Spinner EM, Shannon P, Buice D, Jimenez JH, Veledar E, Del Nido PJ, et al. In vitro characterization of the mechanisms responsible for functional tricuspid regurgitation. Circulation. 2011;124(8):920–9.
4. Hinderliter AL, Willis PWt, Long WA, Clarke WR, Ralph D, Caldwell EJ, et al. Frequency and severity of tricuspid regurgitation determined by Doppler echocardiography in primary pulmonary hypertension.

Am J Cardiol. 2003;91(8):1033–7, A9.

5. Nath J, Foster E, Heidenreich PA. Impact of tricuspid regurgitation on long-term survival. J Am Coll Cardiol. 2004;43(3):405–9.
6. Medvedofsky D, Aronson D, Gomberg-Maitland M, Thomeas V, Rich S, Spencer K, et al. Tricuspid regurgitation progression and regression in pulmonary arterial hypertension: implications for right ventricular and tricuspid valve apparatus geometry and patients outcome. Eur Heart J Cardiovasc Imaging. 2017;18(1):86–94.
7. Menzel T, Kramm T, Wagner S, Mohr-Kahaly S, Mayer E, Meyer J. Improvement of tricuspid regurgitation after pulmonary thromboendarterectomy. Ann Thorac Surg. 2002;73(3):756–61.
8. Sadeghi HM, Kimura BJ, Raisinghani A, Blanchard DG, Mahmud E, Fedullo PF, et al. Does lowering pulmonary arterial pressure eliminate severe functional tricuspid regurgitation? Insights from pulmonary thromboendarterectomy. J Am Coll Cardiol. 2004;44(1):126–32.
9. Lancellotti P, Tribouilloy C, Hagendorff A, Popescu BA, Edvardsen T, Pierard LA, et al. Recommendations for the echocardiographic assessment of native valvular regurgitation: an executive summary from the European Association of Cardiovascular Imaging. Eur Heart J Cardiovasc Imaging. 2013;14(7):611–44.
10. Waziri F, Mellemkjaer S, Clemmensen TS, Hjortdal VE, Ilkjaer LB, Nielsen SL, et al. Long-term changes of resting and exercise right ventricular systolic performance in patients with chronic thromboembolic pulmonary hypertension following pulmonary thromboendarterectomy - A two-dimensional and three-dimensional echocardiographic study. Echocardiography. 2019;36(9):1656–65.
11. Waziri F, Ringgaard S, Mellemkjaer S, Bogh N, Kim WY, Clemmensen TS, et al. Long-term changes of right ventricular myocardial deformation and remodeling studied by cardiac magnetic resonance imaging in patients with chronic thromboembolic pulmonary hypertension following pulmonary thromboendarterectomy. Int J Cardiol. 2020;300:282–8.
12. Galie N, Humbert M, Vachiery JL, Gibbs S, Lang I, Torbicki A, et al. 2015 ESC/ERS Guidelines for the diagnosis and treatment of pulmonary hypertension: The Joint Task Force for the Diagnosis and Treatment of Pulmonary Hypertension of the European Society of Cardiology (ESC) and the European Respiratory Society (ERS): Endorsed by: Association for European Paediatric and Congenital Cardiology (AEPC), International Society for Heart and Lung Transplantation (ISHLT). Eur Heart J. 2016;37(1):67–119.
13. Jensen H, Jensen MO, Ringgaard S, Smerup MH, Sorensen TS, Kim WY, et al. Geometric determinants of chronic functional ischemic mitral regurgitation: insights from three-dimensional cardiac magnetic resonance imaging. J Heart Valve Dis. 2008;17(1):16–22. discussion 3.
14. Trip P, Kind T, van de Veerdonk MC, Marcus JT, de Man FS, Westerhof N, et al. Accurate assessment of load-independent right ventricular systolic function in patients with pulmonary hypertension. J Heart Lung Transplant. 2013;32(1):50–5.

15. Sanz J, Garcia-Alvarez A, Fernandez-Friera L, Nair A, Mirelis JG, Sawit ST, et al. Right ventriculo-arterial coupling in pulmonary hypertension: a magnetic resonance study. Heart. 2012;98(3):238–43.
16. Rolf A, Rixe J, Kim WK, Borgel J, Mollmann H, Nef HM, et al. Right ventricular adaptation to pulmonary pressure load in patients with chronic thromboembolic pulmonary hypertension before and after successful pulmonary endarterectomy–a cardiovascular magnetic resonance study. J Cardiovasc Magn Reson. 2014;16:96.
17. Mutlak D, Lessick J, Reisner SA, Aronson D, Dabbah S, Agmon Y. Echocardiography-based spectrum of severe tricuspid regurgitation: the frequency of apparently idiopathic tricuspid regurgitation. J Am Soc Echocardiogr. 2007;20(4):405–8.
18. Topilsky Y, Khanna A, Le Tourneau T, Park S, Michelena H, Suri R, et al. Clinical context and mechanism of functional tricuspid regurgitation in patients with and without pulmonary hypertension. Circ Cardiovasc Imaging. 2012;5(3):314–23.
19. Sukmawan R, Watanabe N, Ogasawara Y, Yamaura Y, Yamamoto K, Wada N, et al. Geometric changes of tricuspid valve tenting in tricuspid regurgitation secondary to pulmonary hypertension quantified by novel system with transthoracic real-time 3-dimensional echocardiography. J Am Soc Echocardiogr. 2007;20(5):470–6.
20. Afilalo J, Grapsa J, Nihoyannopoulos P, Beaudoin J, Gibbs JS, Channick RN, et al. Leaflet area as a determinant of tricuspid regurgitation severity in patients with pulmonary hypertension. Circ Cardiovasc Imaging. 2015;8(5).
21. Spinner EM, Lerakis S, Higginson J, Pernetz M, Howell S, Veledar E, et al. Correlates of tricuspid regurgitation as determined by 3D echocardiography: pulmonary arterial pressure, ventricle geometry, annular dilatation, and papillary muscle displacement. Circ Cardiovasc Imaging. 2012;5(1):43–50.
22. Park YH, Song JM, Lee EY, Kim YJ, Kang DH, Song JK. Geometric and hemodynamic determinants of functional tricuspid regurgitation: a real-time three-dimensional echocardiography study. Int J Cardiol. 2008;124(2):160–5.
23. Najib MQ, Vinales KL, Vittala SS, Challa S, Lee HR, Chaliki HP. Predictors for the development of severe tricuspid regurgitation with anatomically normal valve in patients with atrial fibrillation. Echocardiography. 2012;29(2):140–6.
24. Utsunomiya H, Itabashi Y, Mihara H, Berdejo J, Kobayashi S, Siegel RJ, et al. Functional Tricuspid Regurgitation Caused by Chronic Atrial Fibrillation: A Real-Time 3-Dimensional Transesophageal Echocardiography Study. Circ Cardiovasc Imaging. 2017;10(1).
25. Baumgartner H, Falk V, Bax JJ, De Bonis M, Hamm C, Holm PJ, et al. 2017 ESC/EACTS Guidelines for the management of valvular heart disease. Eur Heart J. 2017;38(36):2739–91.
26. Kim NH, Delcroix M, Jais X, Madani MM, Matsubara H, Mayer E, et al. Chronic thromboembolic pulmonary hypertension. Eur Respir J. 2019;53(1).

# Figures

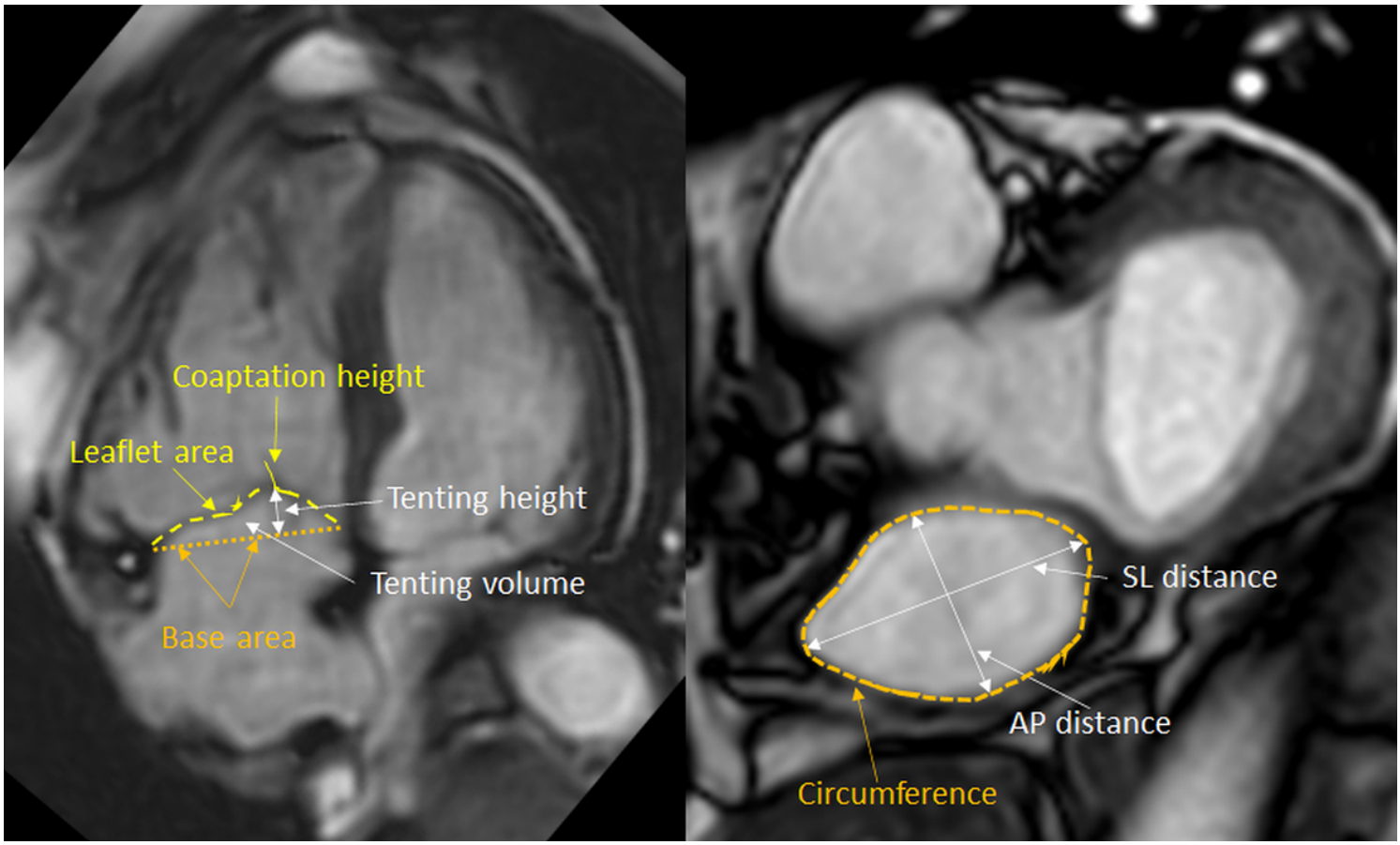


**Figure 1**

CMR images used for detailed analyses of the tricuspid valve. Left panel. Modified 4-chamber view illustrating the definition of coaptation height, leaflet area, tenting height, tenting volume, base area. Right panel. Modified short axis view illustrating the definition of circumference, AP distance, SL distance.

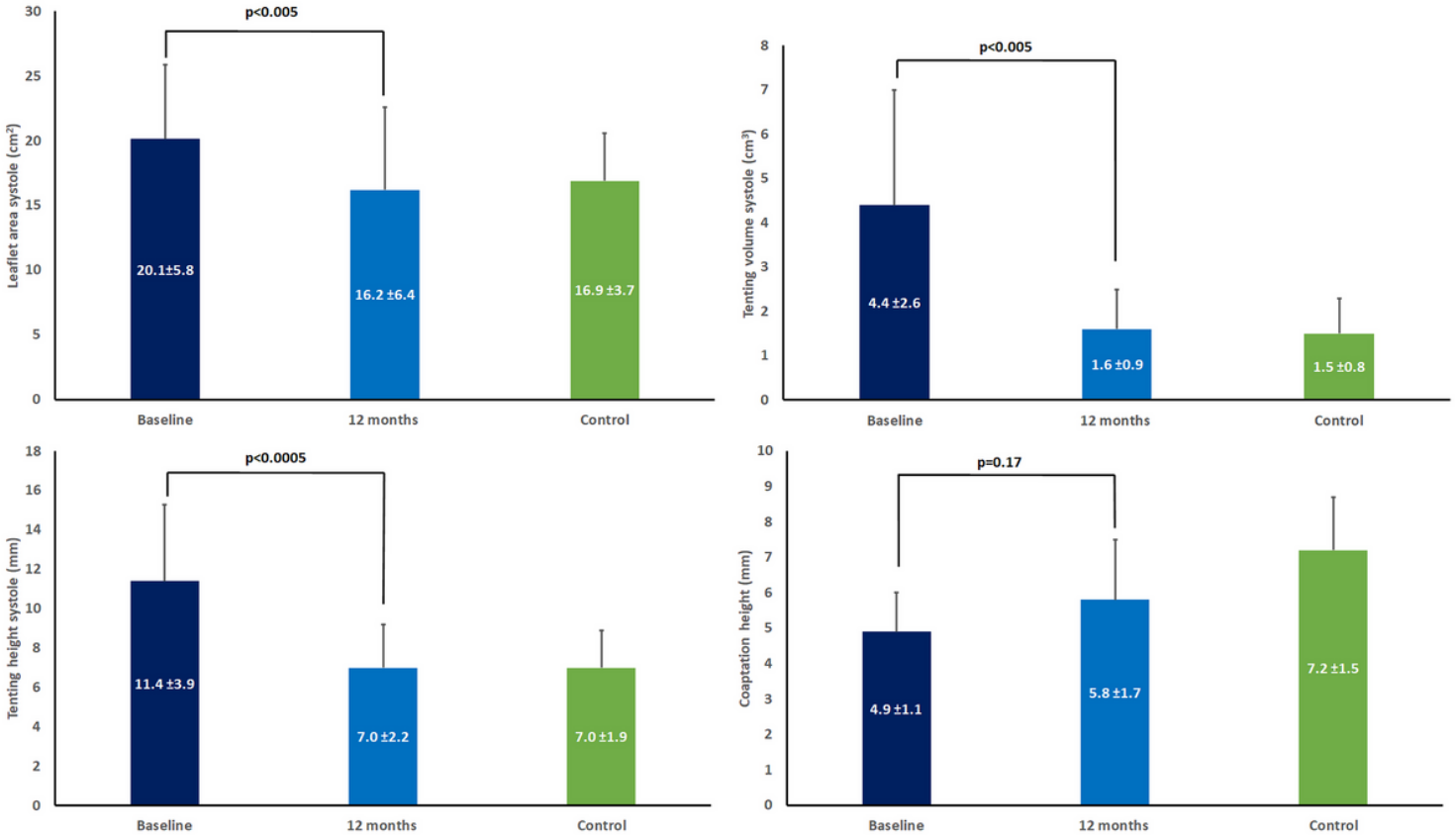


## Figure 2

Key parameters from assessment of the tricuspid valve before and after intervention compared to controls. Upper right panel. Leaflet area in systole. Lower right panel. Tenting height in systole. Upper left panel. Tenting volume in systole. Lower left panel. Coaptation height.